Design and Implementation of a Negative Feedback Oscillator Circuit Based on a Cellular Neural Network with an Opposite Sign Template

BARAN TANDER[1], ATİLLA ÖZMEN[2], YASİN ÖZCELEP[3]

[1]Electronic Communication Technology Program
Kadir Has University
Vocationary School of Technical Sciences, 34590 Silivri/İSTANBUL
TURKEY
tander@khas.edu.tr
[2]Department of Electronics Engineering
Kadir Has University
School of Engineering, 34083 Fatih/İSTANBUL
TURKEY
aozmen@khas.edu.tr
[3]Department of Electrical&Electronics Engineering
İstanbul University
School of Engineering, 34320 Avcılar/İSTANBUL
TURKEY.
ycelep@istanbul.edu.tr

Abstract: - In this paper, explicit amplitude and frequency expressions for a Cellular Neural Network with an Opposite-Sign Template (CNN-OST) under oscillation condition are derived and a novel inductorless oscillator circuit with negative feedbacks, based on this simple structure is designed and implemented. The system is capable of generating quasi-sine signals with tuneable amplitude and frequency which can't be provided at the same time in the classical oscillator circuits.

Key-Words: - Oscillator Circuits, Cellular Neural Networks, Quasi-Sine Signals, Curve and Surface Fitting, Operational Amplifiers, Circuit Design.

1 Introduction

Oscillators are electronic circuits that produce periodical signals (sinusoids, square waves etc.), which play very important roles, especially in communication systems. Colpitts/Hartley, Phase-shift and Wien are widely used sinusoidal oscillator types [1]. The block diagram of a conventional sinusoidal oscillator is shown in Fig. 1.
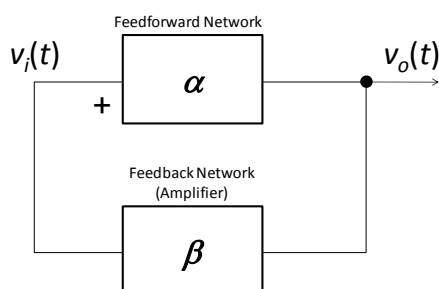

Fig. 1: Block diagram of a conventional sinusoidal oscillator.

Here, the $v_o(t)$ is the periodical output voltage, $v_i(t)$ is the feedback voltage. $\alpha = \dfrac{v_o(t)}{v_i(t)}$ is the voltage gain of the feedforward, $\beta = \dfrac{v_i(t)}{v_o(t)}$ is the voltage gain of the feedback networks. The operation principle is as follows:

The noise in the medium which can be considered as the initial condition $v_o(0)$ for the output voltage, is captured and amplified by the feedforward block employing an active component such as a transistor or an Operational Amplifier (OpAmp), while a 180° phase shift is realized by the passive positive feedback network, until a periodical sine with constant amplitude and frequency is generated as shown in Fig. 2. The feedback network also sets the frequency of the output signal.
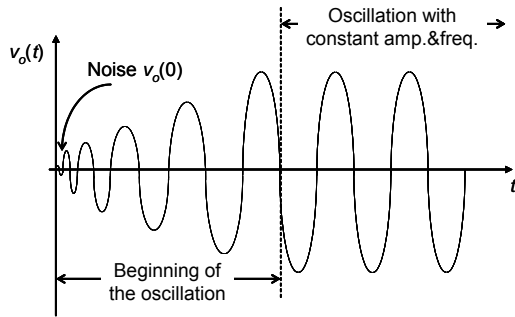
Fig. 2: Operation principle
of a sinusoidal oscillator.

The oscillation constraint is strict $(\alpha \cdot \beta = 1)$ and is determined by voltage gains of both blocks. It can be set to a greater value, however in this case the active component at the feedforward network will saturate. Therefore, the amplitude of oscillation depends only to the source voltage of the active component. Despite the system proposed in this paper, in classical oscillators, the tuning of the amplitude by varying the values of circuit components is not possible because of the positive feedback.

Papers about negative feedback oscillators also exist in literature [2], however our system depends on a Cellular Neural Network (CNN) architecture, therefore having a simpler design, since it only contains fundamental OpAmp application blocks.

The paper is organized as follows; first, a brief information about the CNNs are given and a special CNN system, CNN-OST and its oscillation constraint are introduced. The amplitude and frequency surfaces with respect to template elements are sketched and two explicit analytical approaches are found for each. Secondly, a circuit based on this simple topology is designed, simulated and implemented. The output voltages are compared with the numerical solutions of the nonlinear differential equation system defining the structure. Finally, the advantages and drawbacks of the proposed circuit and future works that can be done are discussed.

2   CNNs
2.1.   CNNs and Their Applications
CNNs are a class of dynamical neural networks and were first proposed by Chua and Yang [3] which

find very effective applications in image processing [4], as well as in chaotic signal generation because of their nonlinear manner [5]. The block diagram of a CNN neuron (cell) is sketched in Fig. 3.
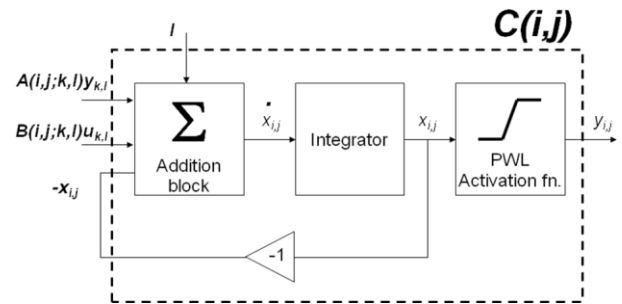

Fig. 3: Block diagram of a CNN cell.

As a dynamic neural network, CNN cells include an integration unit, however unlike the Hopfield nets, here, cells only interact with each other by the r neighbourhood definition given below:

$$N_{ij} = \left\{ C_{kl} \middle| \max \left\{ |k-i|, |l-j| \right\} \le r; 1 \le k \le M, 1 \le l \le N \right\} \quad (1)$$

According to (1), at a neighbourhood dimension of $r = 1$, a cell will only interact with its nearest neighbours. This constraint will dramatically decrease the number of weight coefficients between cells C_{ij} and C_{kl} at an MxN-cell system, enabling a simple implementation. The nonlinear differential equation for a CNN cell $C(i,j)$ shown in Fig. 3 is given by,

$$\dot{x}_{i,j} = -x_{i,j} + A(i,j;k,l)y_{k,l} + B(i,j;k,l)u_{k,l} + I \quad (2)$$

Where $x_{i,j}$ is the "state" of the cell $C(i, j)$ which we will mostly deal throughout the paper; $y_{k,l}$ is the "output", $u_{k,l}$ is the "input" of its neighbour $C(k,l)$; $A(i, j; k\ l)$ is the "weight coefficient" between $C(i, j)$ and the output of $C(k,l)$; $B(i,j;k,l)$ is another "weight coefficient" between $C(i, j)$ and the input of $C(k,l)$; and finally, I is a "threshold" value common for all cells. The activation function namely, "Piecewise Linear Function" (PWL) shown in Fig. 4 can be written as follows

$$y_{i,j} = \frac{1}{2} \left[\left| x_{i,j} + 1 \right| - \left| x_{i,j} - 1 \right| \right] \quad (3)$$
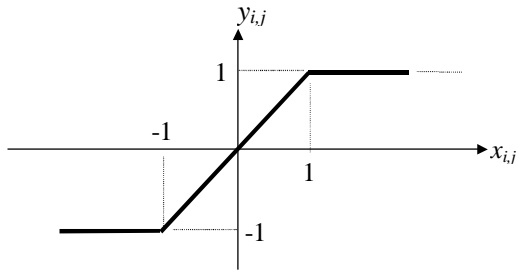
Fig. 4: The PWL activation function of a CNN cell.

The circuit model of the cell $C(i,j)$ is given in Fig. 5. Here, the $v_{xi,j}$ is the "state" $x_{i,j}$; $v_{yi,j}$ is the "output" $y_{i,j}$; $A(i,j;k,l)$ and $B(i,j;k,l)$ are the "weight coefficients" between the cells $C(i,j)$ and $C(k,l)$. The voltage controlled current sources that can easily be realized by OpAmp blocks, and the cascaded non-inverting amplifier and voltage divider at the output providing the PWL activation function, will be discussed at Section 3.1 in detail.
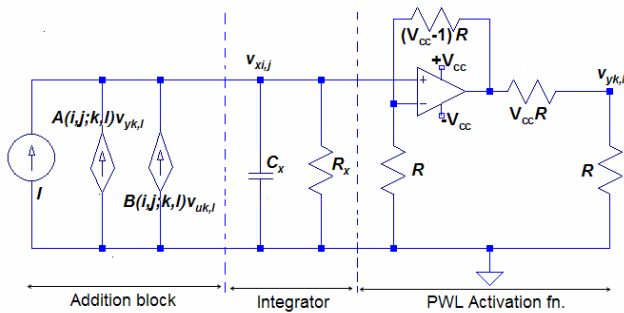

Fig. 5: Circuit model of a CNN cell.

2.2. CNN-OST

Although large number of cells are employed in image processing applications with CNNs [6], a simple version of these networks CNN-OST [7], introduced by Zou and Nossek including only two neurons as seen in Fig. 6 can be used as an oscillator.
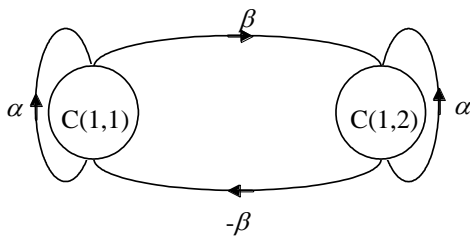

Fig. 6: CNN-OST.

The nonlinear differential equations written in matrix form that define the system is given below:

$$\begin{bmatrix} \dot{x}_1 \\ \dot{x}_2 \end{bmatrix} = -\begin{bmatrix} x_1 \\ x_2 \end{bmatrix} + \underbrace{\begin{bmatrix} \alpha & -\beta \\ \beta & \alpha \end{bmatrix}}_{\mathbf{A}} \cdot \begin{bmatrix} y(x_1) \\ y(x_2) \end{bmatrix} \quad ; \; \alpha > 0 , \beta > 0 \quad (4)$$

Here A is the template matrix that contains the weight coefficients. The α and β are, $A(i,j;i,j)$ the self weight coefficient of a cell and $A(i,j;k,l)$ the weight coefficient with its neighbor, respectively. As seen from (4), the system contains neither $B(i,j;k,l)$ nor I. The x_1 and x_2 solutions can be considered as the outputs. Under oscillation conditions [8], they will have exactly the same amplitude and frequency, however with phase shifts, therefore analyzing only one of them will be sufficient [9].

3 Amplitude and Frequency Surfaces

The variations in **A** change the stability of the system. Savacı and Vanderwelle proved that x_1 and x_2 solutions are oscillations under the following constraint [8]:

$$\beta > \alpha - 1 \quad (5)$$

The oscillations are in quasi-sine waveforms because of the nonlinear characteristic of the PWL activation function. The first goal is to assign explicit formulas for the amplitudes and frequencies of these oscillations with respect to the template components. This process is carried out by sketching the 3D surfaces as functions of αs and βs under the constraint in (5). Mentioned graphics are shown in Fig. 7a and b.
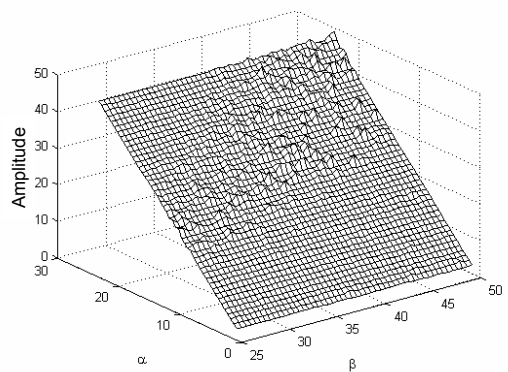
(a)
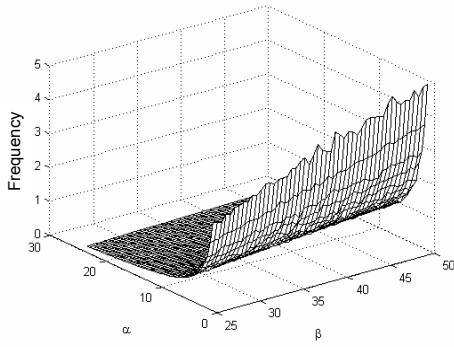
(b)

Fig. 7: (a) Change of amplitude with α and β,
(b) Change of frequency with α and β,
under the constraint given in (5).

As seen from Fig. 7a, the amplitude depends on α and is independent from β, specifically, linearly increasing with α, therefore can be expressed with the form below:

$$G(\alpha)=A\alpha+B \qquad (6)$$

It is clear that, this enables the tuning of the $G(\alpha)$ amplitude by changing the α values. The following A and B coefficients are found by utilizing curve fitting methods within the limitations chosen for the mesh plot:

$$A=2.0013 \qquad (7a)$$
$$B=-0.8332 \qquad (7b)$$

One can see that by analyzing the graphic in Fig. 7b, the frequencies of the oscillations depend on both α and β values. Therefore the following analytical approach will be convinient to describe the dealed parameter:

$$F(\alpha,\beta)=(C/\alpha)\beta+D(\alpha) \qquad (8)$$

Here, the $D(\alpha)$ function is a polynomial with a chosen order of seven which is found by trial and error as the optimum. After a surface fitting process for Fig. 7b, the numerical values for C and the $D(\alpha)$ polynomial are determined as:

$$C=0.14 \qquad (9a)$$
$$D(\alpha)=-1.2651+2.8768\alpha-2.5932\alpha^2+1.2839\alpha^3-$$
$$0.3961\alpha^4+0.0812\alpha^5-0.0115\alpha^6+0.0011\alpha^7 \qquad (9b)$$

These analytical approaches prove that, both amplitudes and frequencies of the signals generated by the system are controllable unlike the conventional oscillators. In order to find the template component values for a chosen amplitude and frequency pair, one must solve the two nonlinear equations (6) and (8) for α and β.

3.   Oscillator Circuit Based on CNN-OST

3.1   Circuit Design

The topology proposed in Fig. 8 is suitable for the realization of the equation system that defines the CNN-OST, where the α and β components are represented by the conductances of the R_α and R_β resistors between the cells [10,11]. The circuit will generate quasi-sine signals under specific component values, however without employing positive feedbacks seen in the conventional oscillator circuits, since all the feedbacks are applied to inverting-inputs of the OpAmps as seen from the schematic. The resistances simulating the components can be computed as follows:

$$R_\alpha = \frac{R_x}{|\alpha|} \qquad (10a)$$

$$R_\beta = \frac{R_x}{|\beta|} \qquad (10b)$$

The node-voltage-equation for the inverting input of the OpAmp Op11 at cell C(1,1), can be written as in (11), if the OpAmp is assumed to be ideal where v_{x1} is the state of this cell, v_{y1} is its output and v_{y2} is the output of the neighbouring cell.

$$\dot{v}_{x1} = \frac{1}{R_x C_x}\left(-v_{x1}+\alpha v_{y1}-\beta v_{y2}\right) \qquad (11)$$

It is clear that by choosing $1/R_x C_x = 1$, the above equation becomes the first row of (4). Here, the Op12-Op13 and Op22-Op23 inverting and non-inverting amplifier pairs provide the PWL characteristics of the activation functions for both cells. In order to obtain the negative β value in (4), an extra inverting amplifier circuitry (Op24) with a gain of "-1" is attached at the output of the cell C(1,2). The quasi-sine oscillations are the v_{x1} and v_{x2} "states" taken from the outputs of the OpAmps Op11 and Op21 providing the load independency as well, since the input resistances of the OpAmps can be assumed as open-circuits.
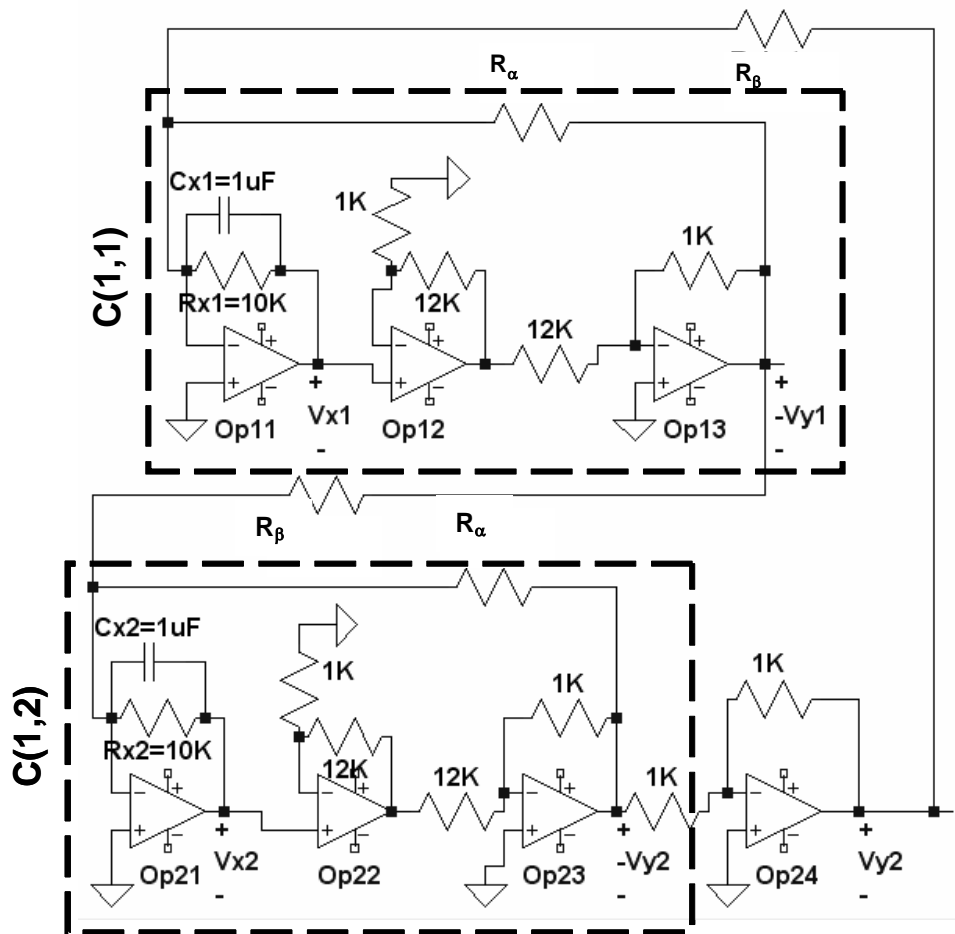
Fig. 8: Proposed oscillator circuit.

3.2.　Frequency Denormalization

The $1/R_x C_x$ coefficient at (11) determines the range of the oscillations' frequency. Specifically, as $1/R_x C_x$ increases the frequency band will increase and decrease vice-versa [12]. By varying either R_x or C_x values, a denormalization process can be carried out by the multiplication of the right hand side of the equation, with the frequency therefore, it is possible to generate oscillations on a wide frequency range without ever changing the resistors for α and β. It is better to vary C_x instead of R_x to achieve this purpose otherwise, as seen from (10), R_α and R_β therefore the mentioned components will be changed for varied R_x values.

One can use stereopotentiometers in order to adjust the values of αs and βs simultaneously, to set the desired amplitude and frequency.

4　Simulation and Implementation

In this section, first, an analysis is performed for a chosen R_α and R_β pair, by comparing the theoretical values of the amplitude and frequency computed by the numerical solutions of (6) and (8) by using a 2-cell CNN model constructed in MatLab Simulink software given in Fig. 9 [11], with the ones obtained from the simulated and implemented circuits. Here, the A and B coefficients in the state equation blocks correspond to $1/R_x C_x$, and the K gains denote the αs and βs between the cells, furthermore Cs and Ds must be chosen as 1 in this model. The PSpice software is used for the circuit simulations. The measurement set up for the implementation is given in Fig. 10.

Then as a synthesis procedure, for a specific amplitude and frequency pair, the design is verified by comparing the measured outputs of the oscillator circuit with the simulation as well as with the numerical solutions of (6) and (8). As depicted

before, the two components of the state set, v_{x1} and v_{x2}, have exactly the same characteristic and waveform however with phase shifts, therefore analyzing a single state (v_{x1}) is enough.
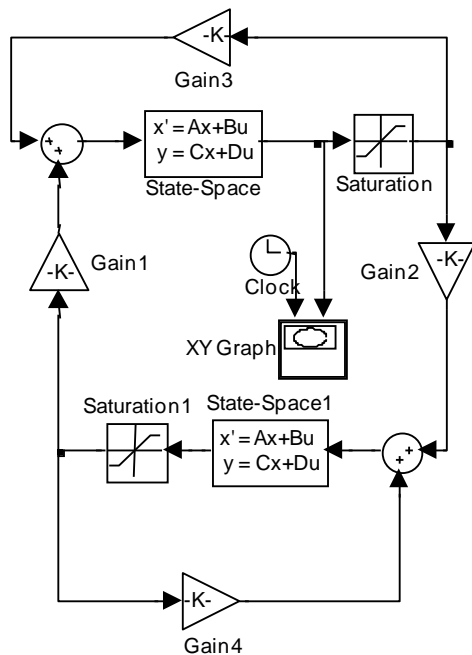

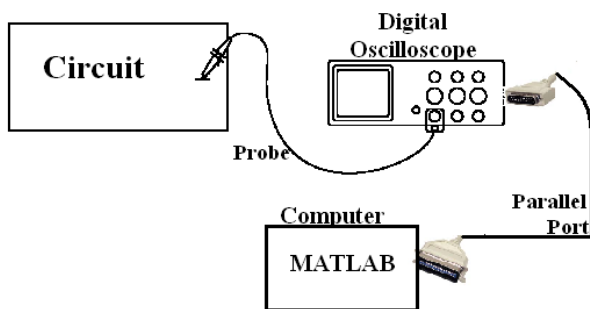**Fig. 9:** The Simulink Model for the CNN based oscillator.

Fig. 10: The measurement set up for implementation.

4.1.   Analysis

If standard resistors R_α =2.2kΩ, R_β=470Ω and R_x=10kΩ are chosen, α and β become 4.545 and 21.276 respectively from (10). Then, by using the analytical approaches given in (6) and (8), the amplitudes and frequencies of the oscillations are computed as, G=7.918V and f=0.625Hz with the model given in Fig. 9. Here, the C_x value is chosen as 1µF, which will denormalize the frequency by $1/R_xC_x$=100 and change it to 62.500Hz as depicted in Section 3.2, for the ease of monitoring the

oscillations with a standard oscilloscope. The piecewise activation relationship between the state and the output of the cell C(1,2) is given in Fig. 12a. The numerical, simulation and implementation results are given in Fig. 11, 12 and 13, respectively.
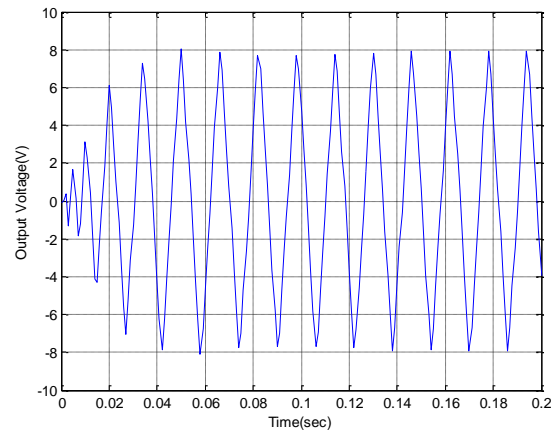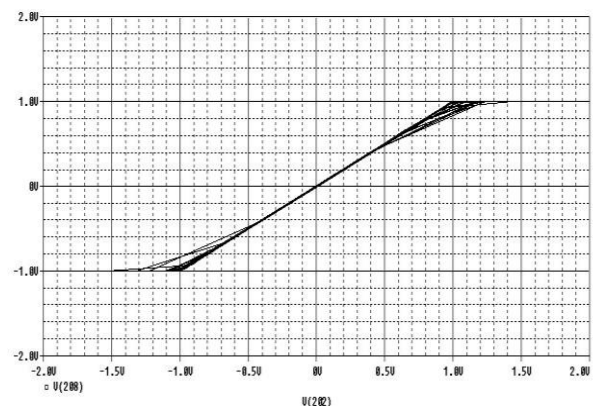

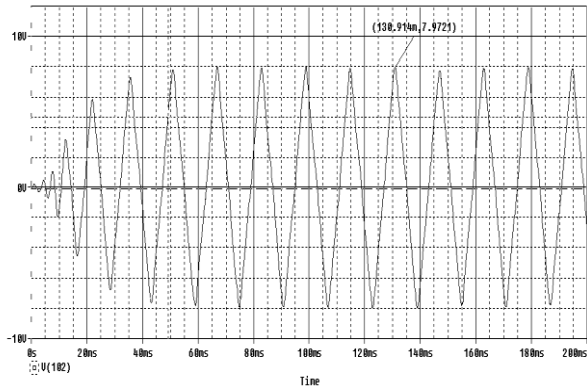**(a)**
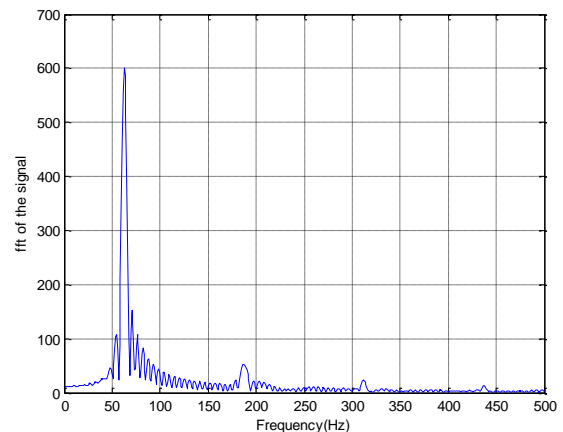
(b)

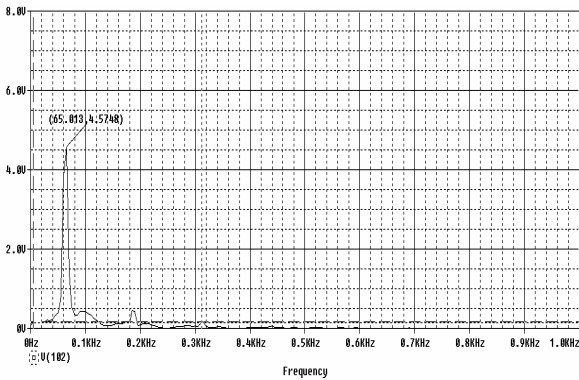**Fig. 11:** The numerical results for the analysis process by using the model given in Fig. 9.
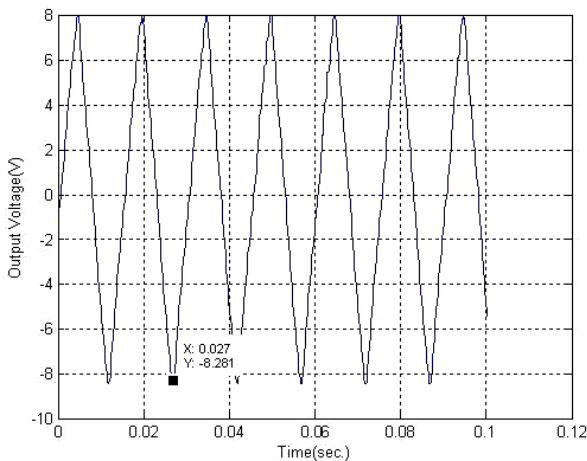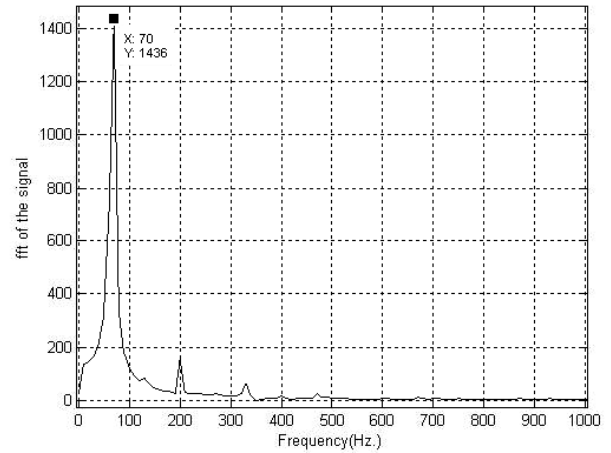(a) Time domain simulation,
(b) Frequency domain simulation.

(a)

(b)

(c)

Fig. 12: Circuit simulations for analysis process:
(a) The simulation of the piecewise linear activation
function at cell C(1,2)
(b) Time-domain simulation,
(c) Frequency domain simulation
for the analysis process when R_α =2.2kΩ, R_β=470Ω.

(a)

(b)

Fig. 13: (a) Implementation result in time domain,
(b) In frequency domain when
R_α =2.2kΩ, R_β=470Ω by using the set up in Fig. 10.

4.2. Synthesis

Here, the amplitude is chosen as G=12V and the frequency as f=1Hz. By solving (6) and (8) simultenously, the α and β values are found as 6.410 and 47.030, which make the corresponding interconnected resistances R_α and R_β 1560.062Ω and 212.630Ω, respectively according to (10). Standard resistors 1500Ω and 220Ω are employed in the simulation and implementation. Moreover, the $1/R_x C_x$ coefficient is made 100 again by choosing R_x=10kΩ and C_x=1μF which will denormalize the oscillation frequency to 100Hz. Numerical, simulation and implementation results in time and frequency domains results are sketched in Fig. 14, 15 and 16.
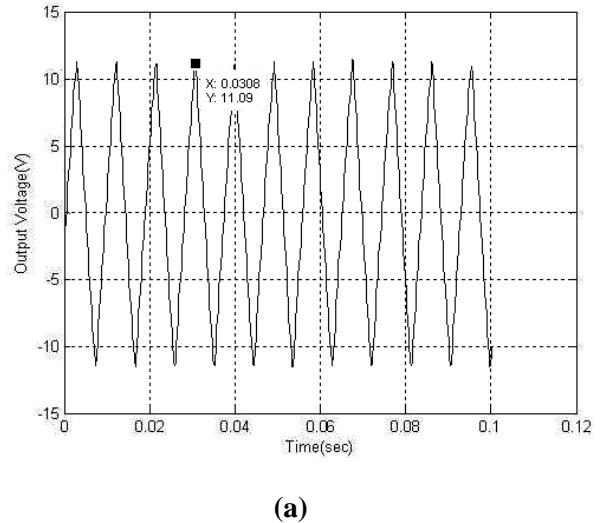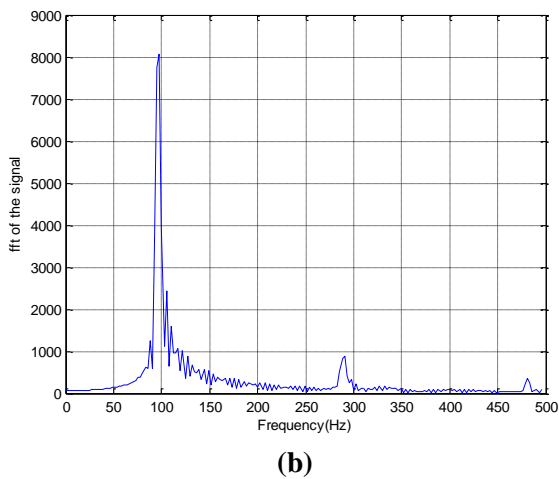

(a)

(b)
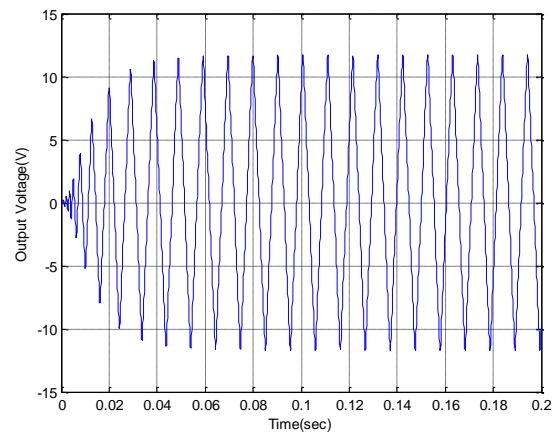
Fig. 14: The numerical results at the synthesis process by using the model given in Fig. 9.
(a) Time domain simulation,
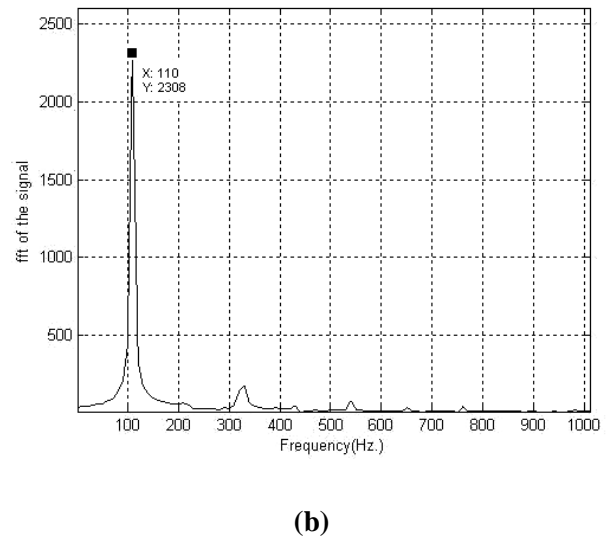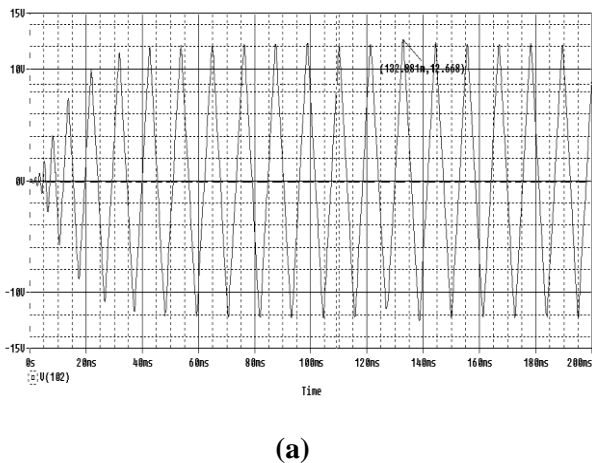**(b)** Frequency domain simulation.
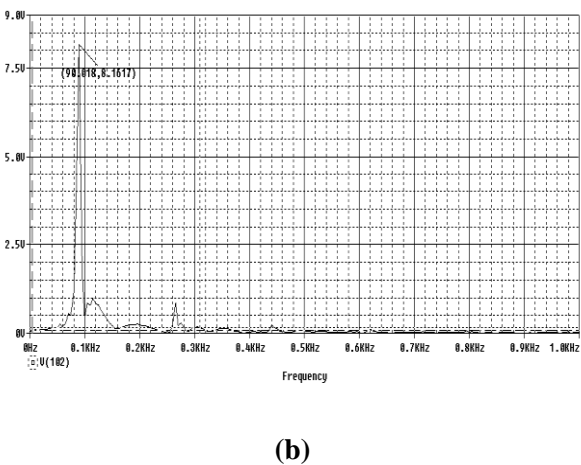

(a)

(b)

Fig. 15: Circuit simulations for synthesis process:
(a) Time-domain simulation,
(b) Frequency domain simulation for chosen amplitude of 12V and frequency of 100Hz

(a)

(b)

Fig. 16: (a) Implementation result in time domain,
(b) In frequency domain for chosen amplitude of 12V and frequency of 100Hz.

Since the oscillations are quasi-sines, one can see that by analyzing all of the frequency domain results, the peak value of the amplitude is not exactly equal to the desired value because of the effect of side harmonics. However, as seen from the operations in time domain, the amplitudes of the oscillations take satisfactory values pretty close to the proposed ones.

Results of the numerical computations, simulations and implementations are summarized in Table-I.

5   Conclusions

In this paper, a CNN based oscillator circuit is designed and implemented. Unlike the classical oscillators, the proposed circuit has negative

Table - I:　　Summary of numerical, simulation and implementation results for analysis and synthesis processes.

Analysis (R_α=2.2kΩ, R_β=470Ω; α=4.545, β=21.276)		
Numerical (Simulink)	**Simulation (PSpice)**	**Implementation**
Amplitude: G=7.918V	G=7.972V	G=8.281V
Frequency: f=62.500Hz	f=65.013Hz	f=70Hz
Synthesis: Amplitude=12V, Frequency=100Hz (α=6.410, β=47.030; R_α=1.5kΩ, R_β=220Ω)		
Numerical (Simulink)	**Simulation (PSpice)**	**Implementation**
G=11.678V	G=12.668V	G=11.090V
f=97.656Hz	f=90.018Hz	f=110Hz

feedbacks and tuneable amplitude. Since it is based on a 1x2-cell structure CNN-OST, it is capable of generating two quasi-sine signals at the same time with phase shifts. Furthermore, the design is inductorless.

The classical 741 BJT OpAmp ICs are employed in the simulation and implementation. If high performance FET OpAmps are used, it is obvious that even more accurate results can be obtained.

Having too many components when compared to conventional oscillators is a drawback, it also seen that the closer the α and β values the worse the output wave shape which must be taken into account in the design. Moreover, because of the nonlinear activation function at the CNN cells, the outputs are not exact sinewaves, therefore contains side harmonics, however, the design is believed to be employed in many applications and suitable for integration.

References:
[1]　Boylestad R., Nashelsky L., *Electronic Devices and Circuit Theory 5th Ed.*, Prentice Hall International Inc., 1992,
[2]　Wang R., Jing Z., Chen L., Periodic Oscillators in Genetic Networks with Negative Feedback Loops, *WSEAS Trans. on Mathematics*, Vol. 3, No. 1, 2004, pp. 150-157,
[3]　Chua L.O., Yang L., Cellular Neural Networks: Theory, *IEEE Trans. CAS*, Vol. 35, No. 10, 1988, pp. 1257–1272,

[4]　Costantini G., Casali D., Carota M., Detection of Moving Objects in 2-D Images Based on a CNN Algorithm and Density Based Spatial Clustering, *WSEAS Trans. on Circuits and Systems*, Vol. 4, No. 5, 2005, pp. 440-447,

[5]　Aissi C., Kazakos D., An Autonoumous Chaotic CNN Hysteresis Circuit, *WSEAS Trans. on Systems*, Vol. 3, No. 1, 2004, pp. 216–220,

[6]　Amanatidis D., Tsaptsinos D., Giaccone P.R., Jones G.A., Image Processing Using CNNs and FPGAs: Initial Results, *NNA2001: WSES International Conference on Neural Network and Applications*, Tenerife, Spain, 2001,

[7]　Zou F., Nossek J.A., Stability of Cellular Neural Networks with Opposite-Sign Templates, *IEEE Trans. CAS*, Vol. 38, No. 6, 1991, pp. 675–677,

[8]　Savaci F.A., Vanderwalle J., On the Stability of Cellular Neural Networks, *IEEE Trans. CAS– I: Fund. Theo. and Apps.*, Vol. 40, No. 3, 1993, pp. 213–215,

[9]　Özmen A., Tander B., A Numerical Method For Frequency Determinatıon in the Astable Cellular Neural Networks with Opposite-Sign Templates, *SIU'06: 14th IEEE Signal Processing and Communication Applications Conference,* Antalya, Turkey, 2006, (In Turkish),

[10]   Tander B., Özmen A., Analytical Approaches for the Amplitude and Frequency Computations in The Astable Cellular Neural Networks With Opposite-Sign Templates, *SIU'07: 15th IEEE Signal Processing and Communication Applications Symposium*, Eskişehir, Turkey, 2007, (In Turkish),

[11]   Tander B., Ün M., Generalized PSPICE and SIMULINK Models for the Continious-Time Simulations of Cellular Neural Networks, *BCSP'2000, 1st IEEE Balkan Conference on Signal Processing, Communications, Circuits and Systems*, Istanbul, Turkey, 2000,

[12]   Tander B., Başkan M., Şenol C., Experimental Analysis of Transients in Low Dimensional Cellular Neural Networks, *ELECO'02: 4th Electronics and Computer Engineering Symposium*, Bursa, Turkey, 2002 (In Turkish).